

Multiparameter Elastic FWI for Quantitative Interpretation: What can be recovered from pressure data?

Guanghui Huang¹, Jaime Ramos-Martínez^{1*}, Carlos Calderón-Macías¹, Faqi Liu¹, and Dan Whitmore¹, introduce a multiparameter elastic FWI formulation directly parameterised in terms of P-wave velocity (v_p), S-wave velocity (v_s), and density (ρ) to assess the extent to which these parameters can be resolved from pressure-only data using a controlled numerical experiment and a field data example of a marine streamer acquisition, with the aim of clarifying their practical interpretability.

Abstract

The expanding application of full-waveform inversion (FWI) beyond structural imaging requires a clearer understanding of which subsurface properties can be robustly recovered from seismic data. Extending FWI from acoustic to elastic formulations enables estimation of parameters critical for quantitative reservoir characterisation. We present a multiparameter elastic FWI (MP-EFWI) workflow for the joint inversion of P-wave velocity (v_p), S-wave velocity (v_s), and density (ρ). As the first-order system of elastodynamic equation is not self-adjoint, an extra adjoint equation is required for computing the correct sensitivity kernels. Our implementation uses the same elastic wave equation for both forward and backward propagation, connected by a compliance tensor for evaluating accurate gradients, avoiding the need for an explicit adjoint solver, thereby improving computational efficiency. The study focuses on pressure-only data typical of marine acquisition. The approach is demonstrated using a synthetic deep-water scenario, where results show that updates in v_s and density are mainly driven by local contrasts, supporting quantitative interpretation. The workflow is then applied to field data offshore Brazil. Inverted models are validated against well-log data and by comparing angle-dependent amplitude responses derived from the inversion with those observed in Kirchhoff prestack depth migration gathers. The results demonstrate that MP-EFWI applied to pressure-only data can provide valuable information to support reservoir characterisation.

Introduction

In velocity model-building and depth imaging, incorporating elastic wave propagation into full-waveform inversion has led to significant improvements. Single-parameter elastic FWI is known to enhance P-wave velocity estimation, particularly in settings with strong impedance contrasts (e.g., Plessix and Krupovnickas, 2021; Liu *et al.*, 2025). As a result, elastic FWI-derived reflectivity (FDR) shows improved resolution in challenging environments such as salt bodies and carbonate

formations, supporting more reliable imaging in areas critical for exploration and development.

Multiparameter elastic FWI (MP-EFWI) further extends these capabilities beyond structural imaging towards quantitative interpretation. Recent studies across different acquisition types and geological settings have demonstrated its potential for estimating subsurface properties relevant to reservoir characterisation and potentially for decision-making in areas with limited well control (e.g., Gomes *et al.*, 2025; Shen *et al.*, 2025). Huang *et al.* (2026) showed that density contrasts, often negatively correlated with P- and S-wave velocity contrasts, can be recovered consistently with amplitude-versus-angle (AVA) anomalies. Their formulation expresses the elastodynamic wave equation in terms of P-wave velocity and reflectivity, reducing parameter trade-offs through gradient scale separation (e.g., Whitmore and Crawley, 2012; Ramos-Martínez *et al.*, 2016). In that framework, density is inferred from inverted reflectivity, while shear velocity contrasts are derived from empirical relationships with P-wave velocity, enabling practical integration with existing interpretation workflows. Shen *et al.* (2025), by contrast, proposed a multiparameter formulation for the joint inversion of P-wave velocity, S-wave velocity, and density, demonstrating that amplitude and phase variations in hydrophone data can be exploited to resolve local variations in all three parameters. This highlights the potential of elastic FWI to extract additional value from conventional marine acquisitions.

Here, we introduce a multiparameter elastic FWI formulation directly parameterised in terms of P-wave velocity (v_p), S-wave velocity (v_s), and density (ρ). We assess the extent to which these parameters can be resolved from pressure-only data using a controlled numerical experiment of a marine streamer acquisition, with the aim of clarifying their practical interpretability. The methodology is then applied to a narrow-azimuth field dataset acquired with dual-sensor technology offshore Brazil. The inverted models are validated against well-log data and further assessed by comparing AVA responses derived from the

¹ TGS

* Corresponding author, E-mail: Jaime.Ramos@tgs.com

DOI: 10.3997/1365-2397.fb2026046

inverted parameters with those observed in Kirchhoff prestack depth migration gathers, demonstrating the applicability of the approach for reservoir characterisation workflows.

Elastic FWI formulation and parameterisation

Elastic full-waveform inversion is commonly formulated using the first-order stress-velocity system. In this framework, a known limitation is that the governing equations are not self-adjoint, requiring a separate adjoint system for gradient computation. This increases both implementation complexity and computational cost. To address this, we adopt a formulation based on the compliance tensor (i.e., the inverse of the stiffness tensor), which allows the adjoint wavefield to be propagated using the same equations as the forward simulation and hence eliminates the need for an explicit adjoint system. As a result, the implementation is simplified. The elastic wave propagation is described by:

$$\rho \frac{\partial v_i}{\partial t} = \frac{\partial \sigma_{ij}}{\partial x_j} \tag{1}$$

$$\frac{\partial \sigma_{ij}}{\partial t} = c_{ijkl} \frac{\partial v_k}{\partial x_l} \tag{2}$$

where v_i is particle velocity, σ_{ij} is the stress tensor, ρ is density, and c_{ijkl} is the stiffness tensor. Within this framework, gradients

of the misfit function with respect to the density and stiffness tensor are expressed as zero-lag correlations between forward and back-propagated wavefields:

$$\nabla_{\rho} J = \int_0^T \frac{\partial v_i}{\partial t} w_i dt \tag{3}$$

$$\nabla_{c_{ijkl}} J = - \int_0^T \frac{\partial v_k}{\partial x_l} S_{ijmn} \tau_{mn} dt \tag{4}$$

where w_i and τ_{ij} are the backpropagated particle velocity and stress fields, and S_{ijmn} is the compliance tensor, respectively. The inversion is parameterised in terms of P-wave velocity (v_p), S-wave velocity (v_s), and density (ρ). The corresponding gradients are obtained via a change of variables using the chain rule and are computed directly within the implementation. From a practical perspective, each parameter influences the data differently. Variations in v_p primarily control kinematics and large-scale impedance contrasts, making it the most robustly constrained parameter. In contrast, v_s and density mainly affect amplitude variations with offset or angle and are therefore more sensitive to local contrasts and data quality. This distinction is particularly important when using pressure-only data, where the absence of direct shear-wave measurements limits the recoverability of elastic parameters. Although the formulation is general, this

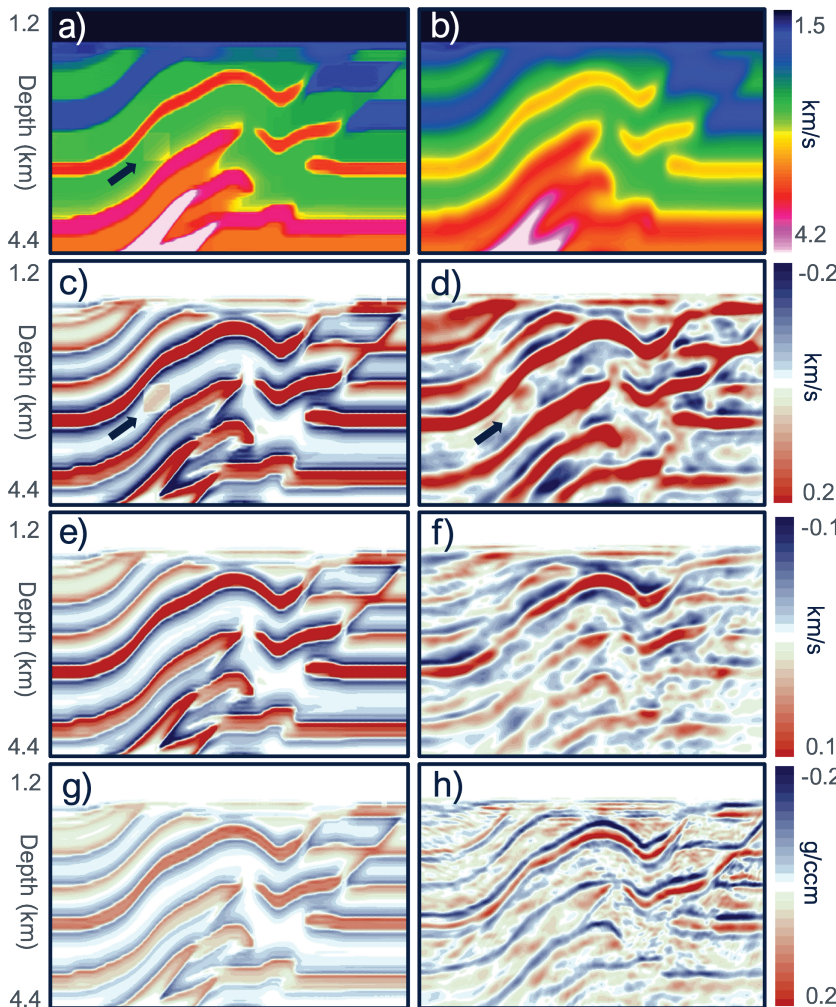


Figure 1 Synthetic example using a modified version of the SEG-EAGE overthrust model. a) True and b) initial model; the initial model is a smoothed version of the true model without the box-shaped inclusion (labelled with the black arrow). The true updates for c) v_p , e) v_s and g) density. Updates for inverted d) v_p , f) v_s and h) density. The true and initial models for the S-wave velocity and density are computed from empirical relations with the P-wave velocity.

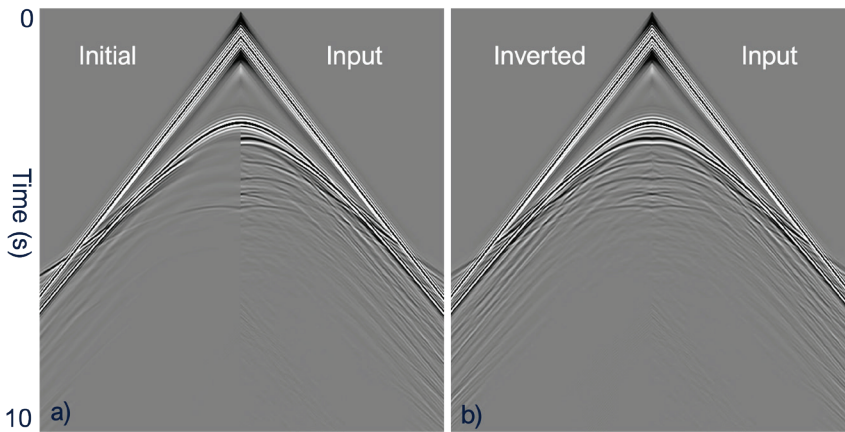


Figure 2 QC validation of the synthetic example. Waveform fit between the input and the modelled traces using the a) initial and b) inverted models.

study focuses on pressure-only data typical of marine streamer acquisitions. This setup enables a direct assessment of v_p , v_s , and density, which helps in clarifying their practical impact for a quantitative interpretation application.

Synthetic example

We assess our approach with a controlled experiment using a modified version of the 3D overthrust model. A water layer is added at the top of the model setting both sources and receivers within it to mimic a streamer acquisition. Figure 1a shows the true v_p model, which contains a box-shaped inclusion, while Figure 1b shows the initial v_p model, a smoothed version of the true model without inclusion. The true and initial v_s models were computed from empirical relations without inclusion. The true density model is built based on Gardner's empirical relation without the inclusion and the initial density is a smoothed version of the true density. The maximum frequency for inversion is 15 Hz, and the maximum

offset is 8 km. In Figures 1c, 1e and 1g, we show the actual difference between true and initial models, while Figures 1d, 1f and 1h show the corresponding inverted v_p , v_s and ρ model updates, respectively, obtained from the simultaneous inversion. The inverted v_p model shown in Figure 1d recovers most of the true update, including the box-shaped anomaly displayed in Figure 1c. The updates for v_p are dominated by lower-wavenumber components compared with those obtained for v_s (Figure 1f). Most of the shear wave velocity information is contained in the recorded compressional amplitudes with kinematics resolved by the P-wave velocity updates. Overall, the v_p model is more accurately resolved than the v_s model. The density (ρ) updates are dominated by high-wavenumber features. This is attributed to the fact that seismic wave propagation does not carry long wavelength information associated with density.

Figure 2 shows the waveform fits of the input data and the modeled data for the initial and inverted models. Notice the

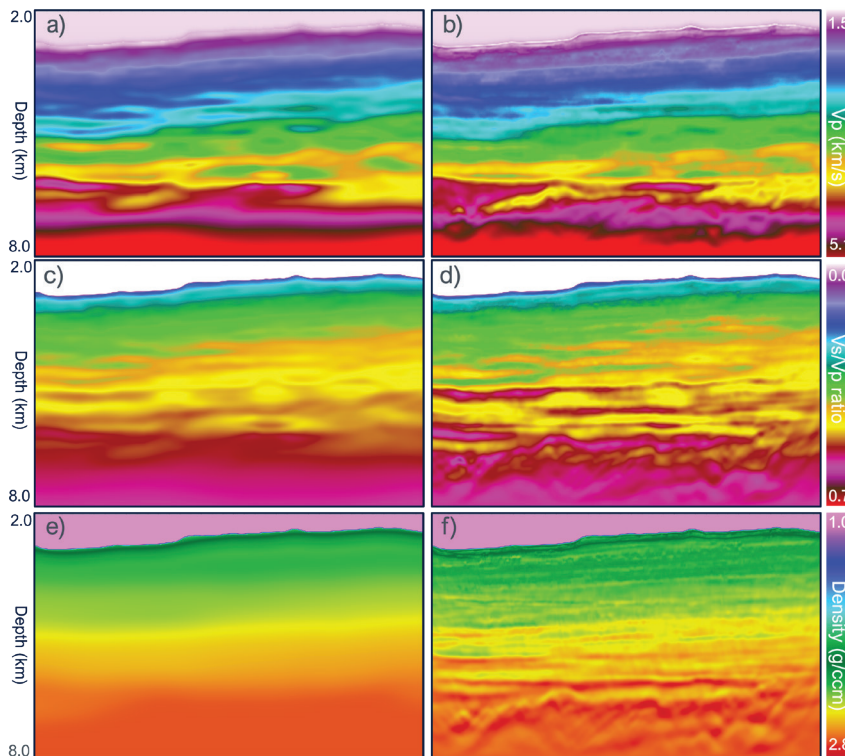


Figure 3 Field data MP-EFWI example in deep-water offshore Brazil. Initial a) v_p , c) v_s/v_p and e) density models. Inverted b) v_p , d) v_s/v_p and e) density models.

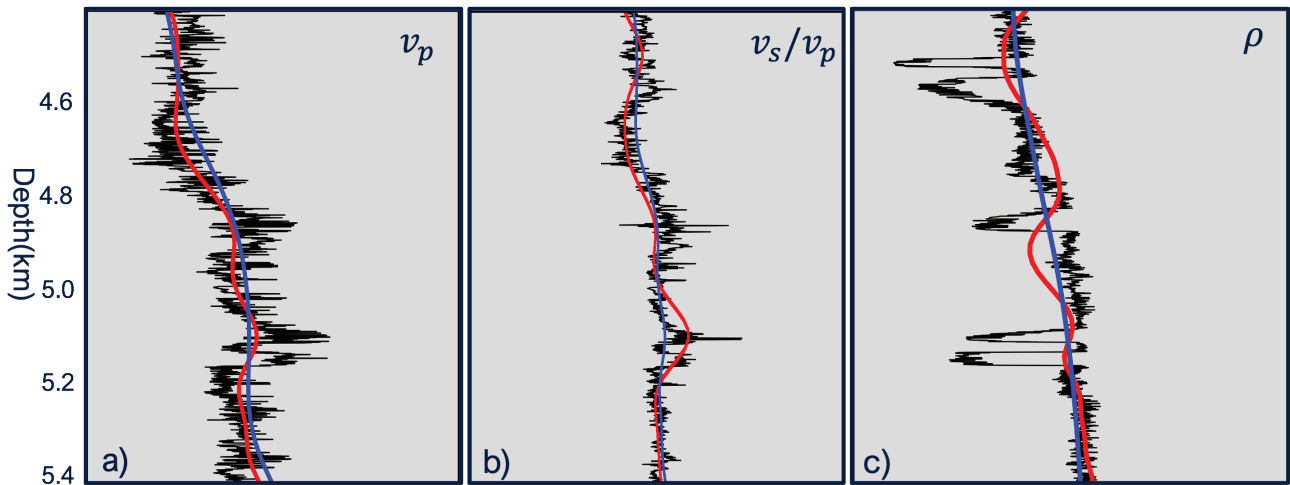


Figure 4 Field data MP-EFVI example in deep-water offshore Brazil. Comparison of the initial (blue line) and inverted (red line) profiles with the well-logs (black line) for a) v_p , b) v_s/v_p and c) density.

excellent match of the events obtained for the modelled traces after the joint inversion of parameters.

Field data application

The proposed MP-EFVI workflow is applied to a narrow-azimuth marine dataset acquired offshore Brazil using dual-sensor streamer technology. The objective is to assess the practical value of the inverted elastic parameters in a real-data setting. Because v_p is the most reliably estimated parameter from P-wave data, the first step focuses on obtaining an accurate P-wave velocity model. The initial v_p model (Figure 3a) was constructed using reflection tomography, which also provided a model for the TTI anisotropic Thomsen parameter ϵ . This model was subsequently improved using MP-EFVI with a P-wave velocity–reflectivity parameterisation as described in Huang *et al.* (2025). A key advantage of this formulation is the scale separation between v_p and reflectivity, which reduces leakage of density effects and minimises high-wavenumber artifacts in the velocity updates. Similar to the approach proposed by Whitmore *et al.* (2021) for acoustic modelling, elastic reflectivity modelling is used during inversion to match the recorded seismic events. The resulting v_p model (Figure 3b) shows good agreement with available sonic logs, indicating that the kinematic components of the data are well explained. Once sufficient accuracy in v_p is achieved, as confirmed by kinematic quality control, not shown for brevity, the inversion strategy shifted to updating v_s and density using the full offset range of the data.

The initial v_s and density models were derived from empirical relationships based on the updated v_p . The initial v_s/v_p ratio is shown in Figure 3c, while the initial density model (Figure 3e) is a strongly smoothed version of the empirical estimate, ensuring independence from high-wavenumber velocity features except at the water-bottom boundary. During this second stage, v_p was held fixed, and density were updated over multiple frequency bands. The inversion results indicate that updates in v_s and density are primarily driven by amplitude and phase variations in the P-wave reflectivity response, and are therefore dominated by localised contrasts, consistent with other published studies (e.g., Shen *et al.*, 2025). The final v_s/v_p model (Figure 3d) and density

model (Figure 3f) exhibit predominantly high-wavenumber features, in agreement with observations from the synthetic experiment. An important observation is that the background (low-wavenumber) components of v_s and density remain largely unchanged after this step. This reflects the limited kinematic sensitivity of P-wave data to these parameters. Instead, the recovered v_s and density variations are spatially correlated with high-wavenumber features in the v_p model, which provides the underlying large-scale structure. This behaviour is expected to be in contrast with inversion results incorporating multi-component data, where longer-wavelength updates to the background model may be achievable from recorded shear-wave arrivals.

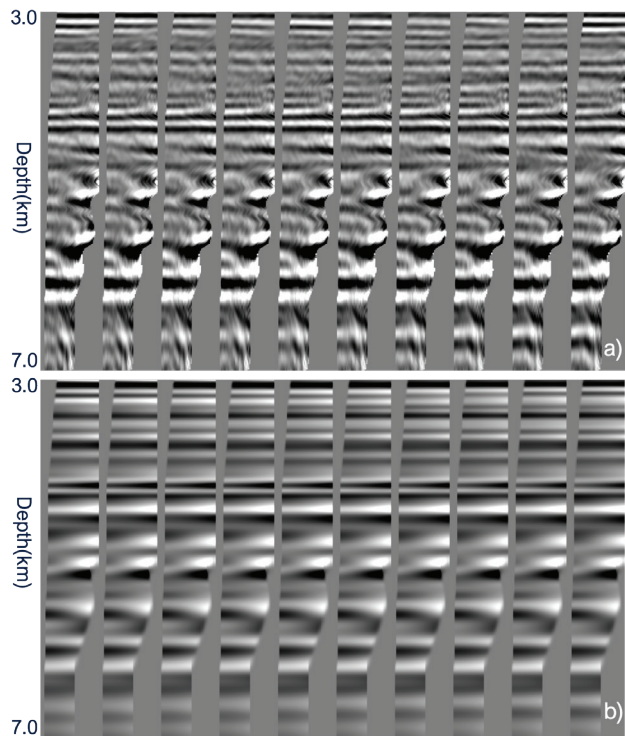


Figure 5 Image gathers computed from a) Kirchhoff depth migration and b) constructed from the MP-EFVI parameters utilising the Aki and Rickards AVA linear approximation.

Figure 4 compares well-log measurements with inverted profiles of v_p , v_s/v_p , and density at a well location. The results show clear improvement relative to the initial models. In particular, the inverted v_p and v_s/v_p profiles are in better agreement with the logs, demonstrating that the inversion captures both kinematic and elastic trends. For density, the inversion recovers localised negative contrasts observed in the well logs, particularly in intervals associated with previously identified as a Class IIp AVA anomaly. As in the synthetic case, the comparison for v_s/v_p and density is most meaningful at shorter wavelengths, reflecting the limited sensitivity of pressure data to their large-scale variations.

To further assess the consistency of the inverted models, angle-dependent reflectivity responses are computed directly from the estimated elastic parameters using the linearised approximation of Aki and Richards (1980). Parameter contrasts ($\Delta v_p/v_p$), ($\Delta v_s/v_s$), and ($\Delta\rho/\rho$) are extracted from the inverted volumes and used to generate synthetic angle gathers up to 45°, depicted in Figure 5a. These responses represent the prestack amplitudes implied by the described MP-EFWI solution. Figure 5b shows Kirchhoff prestack depth-migrated angle gathers at the same location, obtained using the reference model. Despite being derived from fundamentally different workflows, the two sets of gathers display a consistent AVA behaviour. This agreement provides a validation that the inverted elastic parameters capture the key amplitude variations present in the data.

Conclusions

We have presented a multiparameter elastic FWI (MP-EFWI) workflow for the joint inversion of v_p , v_s , and density using pressure-only seismic data. The proposed parameterisation and inversion strategy enable the recovery of localised variations in v_s and density from P-wave reflectivity signatures, extending beyond the conventional estimation of v_p obtained from single-parameter approaches. These estimations provide valuable inputs for quantitative reservoir characterisation. The methodology has been demonstrated on streamer data from deep-water offshore Brazil. The inverted models show good agreement with well-log measurements, supporting the reliability of the recovered elastic parameters. In particular, the results indicate that meaningful information about shear velocity and density can be extracted even in the absence of direct shear-wave measurements. From a practical perspective, two key observations emerge. First, the nonlinear nature of MP-EFWI enables the recovery of elastic information beyond what is typically achieved with conventional linearised AVO analysis, especially in areas with limited well control. Second, the approach avoids several simplifying assumptions commonly used in AVO workflows, such as

locally one-dimensional media after migration, allowing for more consistent interpretation in structurally complex settings. Overall, these results demonstrate that MP-EFWI applied to pressure-only data can provide reliable and interpretable elastic parameters, thereby enhancing reservoir characterisation and supporting a more informed subsurface interpretation.

Acknowledgements

We would like to thank TGS for permission to publish this material. We would also like to thank Multiclient TGS for authorisation to use the field dataset. We thank our colleagues in TGS R&D Geophysics for valuable discussions.

References

- Aki, K. and Richards, P.G. [1980]. *Quantitative Seismology, Theory and Methods*, Vol I. Freeman and Company, San Francisco.
- Gomes, A., Rocha, D., Plessix, R.É., Wong, M., Perkins, C. and Goh, V. [2025]. High-resolution impedance estimation using multiparameter viscoelastic FWI in a Gulf of Mexico setting. *The Leading Edge*, **44**(5), 394-402.
- Huang, G., Macesanu, C., Liu, F., Ramos-Martínez, J., Whitmore, D. and Calderón, C. [2025]. Multiparameter elastic FWI for joint inversion of velocity and reflectivity: 86th EAGE Annual Conference & Exhibition, *Extended Abstracts*.
- Huang, G., Macesanu, C., Liu, F., Ramos-Martínez, J., Calderón, C. and Whitmore, D. [2026]. Multiparameter Elastic Full Waveform Inversion for Reservoir Interpretation: 87th EAGE Annual Conference & Exhibition, *Extended Abstracts*.
- Liu, F., Macesanu, C., Xing, H., Romanenko, M., Zhan, G., Calderón-Macías, C. and Wang, B. [2025]. Elastic full-waveform inversion: Enhance imaging for legacy and modern acquisition. *The Leading Edge*, **44**(5), 338-343.
- Plessix, R.-É. and Krupovnickas, T. [2021]. Low-frequency, long-offset elastic waveform inversion in the context of velocity model building. *The Leading Edge*, **40**(5), 342-347.
- Ramos-Martínez, J., Crawley, S., Zou, K., Valenciano, A.A., Qiu, L. and Chemingui, N. [2016]. A robust gradient for long wavelength FWI updates. 78th EAGE Annual Conference & Exhibition, *Extended Abstracts*.
- Shen, P., Albertin, U., Malcotti, H., Haataja, J. and Sekar, A. [2025]. Feasibility of V_p , V_s , density inversion by elastic FWI. *The Leading Edge*, **44**(5), 403-412.
- Whitmore, D. and Crawley, S. [2012]. Application of RTM inverse scattering imaging conditions. SEG Technical Program, *Expanded Abstracts*.
- Whitmore, N.D., Ramos-Martínez, J., Yang, Y. and Valenciano, A.A. [2020]. Full wave field modelling with vector-reflectivity. 82nd EAGE Annual Conference & Exhibition, *Extended Abstracts*.